

A numerical study on the seepage failure by heave in sheeted excavation pits

Serdar Koltuk*, Tomas M. Fernandez-Steeger and Rafiq Azzam

*Department of Engineering Geology and Hydrogeology, RWTH Aachen University,
Lochnerstr. 4-20, D-52064 Aachen / Germany*

(Received October 31, 2014, Revised June 03, 2015, Accepted July 14, 2015)

Abstract. Commonly, the base stability of sheeted excavation pits against seepage failure by heave is evaluated by using two-dimensional groundwater flow models and Terzaghi's failure criterion. The objective of the present study is to investigate the effect of three-dimensional groundwater flow on the heave for sheeted excavation pits with various dimensions. For this purpose, the steady-state groundwater flow analyses are performed by using the finite element program ABAQUS 6.12. It has been shown that, in homogeneous soils depending on the ratio of half of excavation width to embedment depth b/D , the ratio of safety factor obtained from 3D analyses to that obtained from 2D analyses $FS_{(3D)}/FS_{(2D)}$ can reach up to 1.56 and 1.34 for square and circular shaped excavations, respectively. As failure body, both an infinitesimal soil column adjacent to the wall (Baumgart & Davidenkoff's criterion) and a three-dimensional failure body with the width suggested by Terzaghi for two-dimensional cases are used. It has been shown that the ratio of $FS_{(Terzaghi)}/FS_{(Davidenkoff)}$ varies between 0.75 and 0.94 depending on the ratio of b/D . Additionally, the effects of model size, the shape of excavation pit and anisotropic permeability on the heave are studied. Finally, the problem is investigated for excavation pits in stratified soils, and important points are emphasized.

Keywords: seepage failure; heave; sheeted excavation pit; three-dimensionality; finite element method

1. Introduction

The effect of seepage flow on geotechnical stability problems, such as in natural slopes, embankment dams, tunnel constructions, sheeted excavation pits etc., is manifold (Kaiser and Hewitt 1982, Lee and Nam 2001, Ghiassian and Ghareh 2008, Yang and Qin 2014). The present study focuses on the seepage failure by heave in sheeted excavation pits.

When the depth of a planned excavation pit is lower than the groundwater level in the field, the water level should be lowered to keep the excavation area dry. However, the lowering of groundwater level over a large area is not always possible in urban areas for different reasons: (1) it causes an increase of effective stresses within the soil, and thus, an increase of settlements around the excavation area, which can damage neighboring buildings, underground pipelines and roads. In addition, settlements may appear where the wooden foundation piles of older buildings are exposed to oxygen and begin to rot; (2) the lowering of the groundwater level cannot always be permitted with regard to existing water regulations; (3) the drainage of pumped water may be

*Corresponding author, Ph.D. Student, E-mail: koltuk@lih.rwth-aachen.de

problematic in respect of the capacity of local sewage system.

For the reasons mentioned above, after the construction of impermeable embedded walls, only the groundwater inside the excavation pit is pumped out without affecting the groundwater level outside the excavation pit. However, owing to the developed hydraulic head difference, groundwater flow takes place from the upstream side into the excavation area, which may endanger the stability of the excavation pit.

According to EN 1997-1 / Eurocode 7 (2004), failures induced by seepage flow appear in the form of heave, uplift, internal erosion or piping. Failure by uplift occurs when the pore water pressure at the bottom of an injection slab or an underwater concrete slab, which is constructed to reduce the flow rate into the excavation pit, becomes greater than the overburden pressure due to the weight of the slab and overlying soil layers. The uplift also occurs when the pore water pressure at the bottom of a soil layer that is underlain by a confined aquifer becomes greater than the weight of overlying soil layers. Internal erosion is the transport of soil grains within a soil layer, at the interface of two different soil layers, or at the interface of a soil layer and a structure by groundwater flow, which may finally lead to collapse. Failure by piping is a particular form of the internal erosion where erosion begins with a pipe shaped canal on the downstream side, and propagates backwards. A failure similar to heave occurs as soon as the pipe shaped canal reaches the ground surface on the upstream side, as shown in Fig. 1.

Heave appears when the pore water pressure developed by groundwater flow lifts the soil on the downstream side. This phenomenon in cohesionless soils has been investigated by several researchers, and various verification methods have been developed (Terzaghi 1925, Terzaghi and Peck 1948, Harza 1935, McNamee 1949, Marsland 1953, Davidenkoff and Franke 1965, Davidenkoff 1970, Tanaka and Verruijt 1999, Benmebarek *et al.* 2005, Ziegler *et al.* 2009, Zheng and Yang 2011, Aulbach and Ziegler 2014).

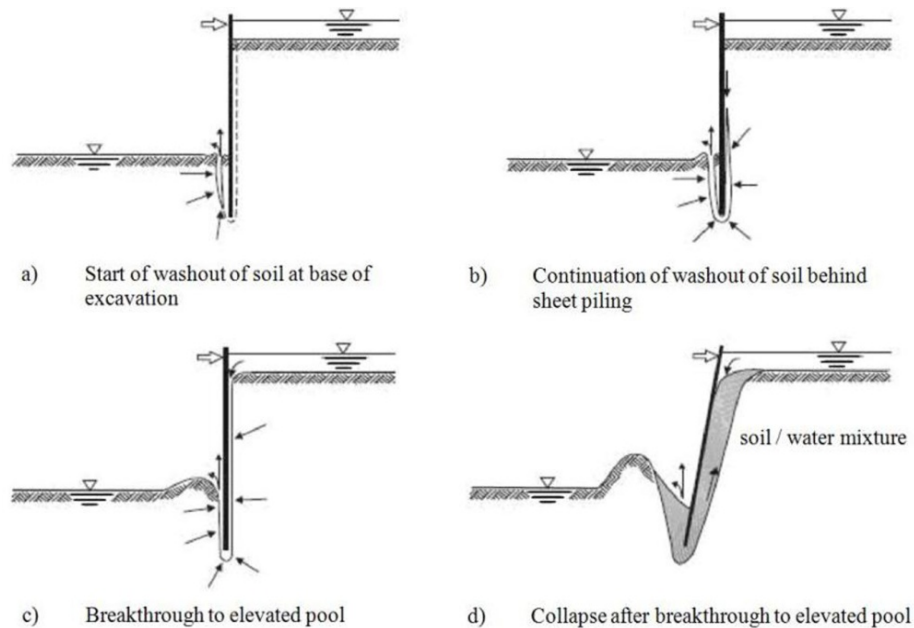


Fig. 1 Development of piping around waterfront structures (EAU 2004)

The most common verification method was presented by Terzaghi (Terzaghi 1925, Terzaghi and Peck 1948). He found from two-dimensional model tests with homogeneous soils that the heave zone lifted by pore water pressure develops in the form of a rectangular prism. The height and width of this prism are equal to the embedment depth D of the wall and its half $D/2$, respectively. For the verification of heave, the average pore water pressure at the bottom of the heave zone $(u_1 + u_2)/2$ is equated to the total stress at the same level (see Fig. 2). It gives Eq. (1)

$$\frac{\Delta h_2}{D} = \frac{\gamma_{sat} - \gamma_w}{\gamma_w} \tag{1}$$

where Δh_2 is the difference between the average hydraulic head at the bottom level of the heave zone and the hydraulic head on the excavation base, γ_{sat} and γ_w are the unit weights of saturated soil and water, respectively. The ratios of $\Delta h_2 / D$ and $(\gamma_{sat} - \gamma_w) / \gamma_w$ are called the average hydraulic gradient according to Terzaghi’s approach $i_{Terzaghi}$ and the critical hydraulic gradient i_{cr} , respectively.

Marsland (1953) reported that seepage failure in loose sands occurs when the pore water pressure at the wall tip becomes equal to the total stress at the same level. Based on the results of one-dimensional seepage experiments, Fellin *et al.* (2003) suggested to use Baumgart & Davidenkoff’s method in loose sands in which seepage failure appears at hydraulic gradients smaller than critical hydraulic gradient. EAU (2004) “Recommendations of the committee for waterfront structures, harbours and waterways” and EAB (2008) “Recommendations on excavations” point out Baumgart & Davidenkoff’s method in addition to Terzaghi’s method.

Davidenkoff (Davidenkoff and Franke 1965, Davidenkoff 1970) stated that, with regard to hydraulic heave, the stability of the infinitesimal soil column adjacent to the wall is decisive. This method considers the maximum pore water pressure, which occurs at the wall tip on the downstream side. Accordingly, it gives the minimum possible safety factor against heave. For the verification of heave, the pore water pressure at the wall tip u_1 is equated to the total stress at the same level (see Fig. 2). It gives Eq. (2)

$$\frac{\Delta h_1}{D} = \frac{\gamma_{sat} - \gamma_w}{\gamma_w} \tag{2}$$

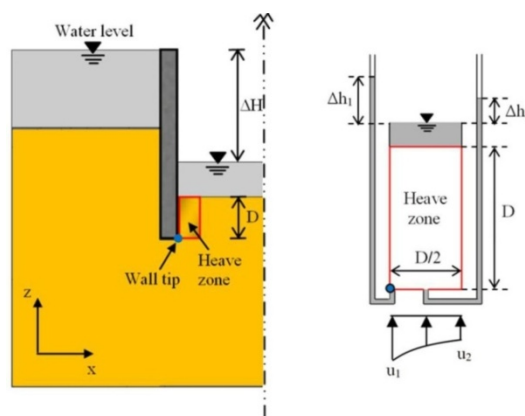


Fig. 2 Verification against seepage failure by heave

where the ratio of $\Delta h_1/D$ is the average hydraulic gradient along the soil column with infinitely small width adjacent to the wall. In this study, $\Delta h_1/D$ is called the maximum hydraulic gradient i_{\max} (or $i_{\text{Davitenkoff}}$) although even larger gradients occur near the wall tip on the downstream side.

The critical hydraulic gradient can be also given through the specific gravity of soil particles G_s and the void ratio of soil e as follows

$$i_{cr} = \frac{\gamma_{sat} - \gamma_w}{\gamma_w} = \frac{G_s - 1}{e + 1} \quad (3)$$

An average hydraulic gradient that is equal to or larger than i_{cr} leads to hydraulic heave. The value of i_{cr} varies within a range of about 0.80-1.20 for most cohesionless soils. High plasticity soils do not necessarily become quick at zero effective stress as they retain their strengths through cohesion even at zero effective stress. Thus, the critical hydraulic gradient for a cohesive soil is greater than that calculated from Eq. (3) (Wudtke and Witt 2006). The exception is in the case of dispersive clays, where interparticle bonds are weak and are easily influenced by changes in the chemistry of eroding fluid (Reddi 2003). Furthermore, an average hydraulic gradient slightly greater than i_{cr} occurring at the bottom level of a dispersive or non-dispersive cohesive layer can lead to seepage failure by uplift if the base of the cohesive soil layer, which is underlain by a relatively more permeable cohesionless soil layer, is located between the wall tip and the excavation base.

It should be mentioned that the actual field conditions may differ from the assumed theoretical model. Geologic defects, inadequately sealed boreholes, etc., can significantly alter the flow regime. Therefore, the stability computations are only approximate and should be compensated using a safety factor ($FS = i_{cr}/i_{\text{Terzaghi}}$ or $i_{cr}/i_{\text{Davitenkoff}}$). Generally, a safety factor of 1.5 is recommended against heave (EN 1997-1 / Eurocode 7, 2004).

Eq. (3) is valid when the groundwater level lies on or above the excavation base. In the field, the groundwater level is kept to 0.5-1 m below the excavation base for safety reasons. In this case, the critical hydraulic gradient i_{cr} is derived as

$$i_{cr} = \frac{d\gamma + D(\gamma_{sat} - \gamma_w)}{D\gamma_w} \quad (4)$$

where d is the distance between the excavation base and the groundwater level on the downstream side, D is the embedment depth of the wall below the groundwater level, and γ is the moisture unit weight of soil. Eq. (4) gives a larger critical hydraulic gradient than that calculated from Eq. (3), especially for excavation pits with small embedment depths.

Commonly, the average hydraulic gradient $\Delta h_1/D$ (or $\Delta h_2/D$) is determined by drawing a flow net, which is a graphical method to solve two-dimensional Laplace's equation given below

$$k_x \frac{\partial^2 h}{\partial x^2} + k_z \frac{\partial^2 h}{\partial z^2} = 0 \quad (5)$$

where k_x and k_z are the hydraulic conductivities of soil, $\partial h/\partial x$ and $\partial h/\partial z$ are the hydraulic gradients in any point within the flow zone in horizontal (x) and vertical (z) directions, respectively. The various solution techniques of Eq. (5) can be found in the literature (Harr 1962, Reddi 2003, Das 2008).

However, numerical and experimental studies demonstrated that the hydraulic gradients obtained from three-dimensional models are larger than those obtained from two-dimensional models (Davidenkoff and Franke 1965, Schmitz 1990, Cai *et al.* 2004, Hirosa and Tanaka 2007, Tanaka *et al.* 2012, Aulbach and Ziegler 2013). In this study, a comparison between two- and three- dimensional analyses is given based on the results of steady-state groundwater flow analyses performed by using the finite element program ABAQUS 6.12. This comparison enables users to evaluate the effect of three-dimensional groundwater flow on the hydraulic heave in square and circular shaped sheeted excavation pits with various dimensions. Hydraulic gradients are determined according to Davidenkoff's failure criterion. In order to show the effect of the shape of failure body on hydraulic heave, the hydraulic gradients ($i_{\text{Davidenkoff}}$) are compared with those determined by using a three-dimensional failure body with the width suggested by Terzaghi for two-dimensional cases (i_{Terzaghi}). Additionally, based on the results of three-dimensional analyses, the effects of the factors such as the size of numerical model, the shape of excavation pit, and anisotropic permeability on the hydraulic gradient are studied. Finally, seepage failure by heave is investigated for excavation pits in stratified soils, and important points are emphasized.

2. Numerical investigation

The numerical models in this study consider only a quarter of examined excavation pits taking advantage of symmetry, as shown in Fig. 3a. The dimensions of the soil models (R and T) are chosen such that the boundary effect on the results is negligibly small. R and T represent the horizontal distance from the wall and the vertical distance from the wall base to the outer boundaries of the soil model respectively. The groundwater level on the downstream side, which is shown with the blue-colored surface, lies on the excavation base. The symbols ΔH , D and b in Fig. 3(b) represent the potential difference, the embedment depth of the wall, and half of the excavation width (half of the excavation diameter in the case of a circular shaped excavation), respectively.

The thickness of the impermeable embedded walls is chosen such that its effect on the results is negligibly small. The vertical boundaries and the bottom boundary of the soil models are also impermeable. The deformations of the models that result from the groundwater flow, in other

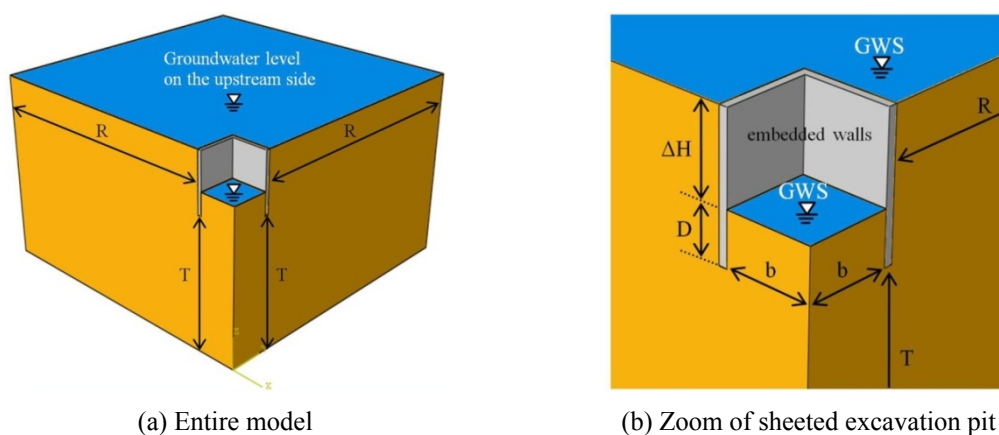


Fig. 3 Numerical model

words from the change of effective stresses, are prevented. The soil is modeled with 8-node brick trilinear displacement/pore pressure elements (C3D8P). The mesh is refined near the wall where the flow gradients are concentrated. The number of elements in the models is chosen such that its effect on the results is negligibly small. Accordingly, it varies between about 19000 and 97000 depending on the model size.

Figs. 4(a) and 5(a) show the equipotential lines (surfaces) for square and circular shaped sheeted excavation pits, respectively. The water level on the downstream side is chosen as the reference water level. Accordingly, the pore pressure boundary condition on the upstream side is set equal to the potential difference ΔH whereas its value on the downstream side is set equal to zero. The horizontal cross sections at the level of the wall base on the downstream side of a square and circular shaped sheeted excavation are shown in Figs. 4(b) and 5(b) respectively. The shown locations of the potential heads are used to verify the safety against heave according to Baumgart & Davidenkoff's and Terzaghi's approaches. The zones lying between the embedded walls and the dashed lines in these figures are considered as the bases of the assumed three-dimensional failure bodies, and the potential heads in the middle of these bases are used to verify the safety against heave according to Terzaghi's method.

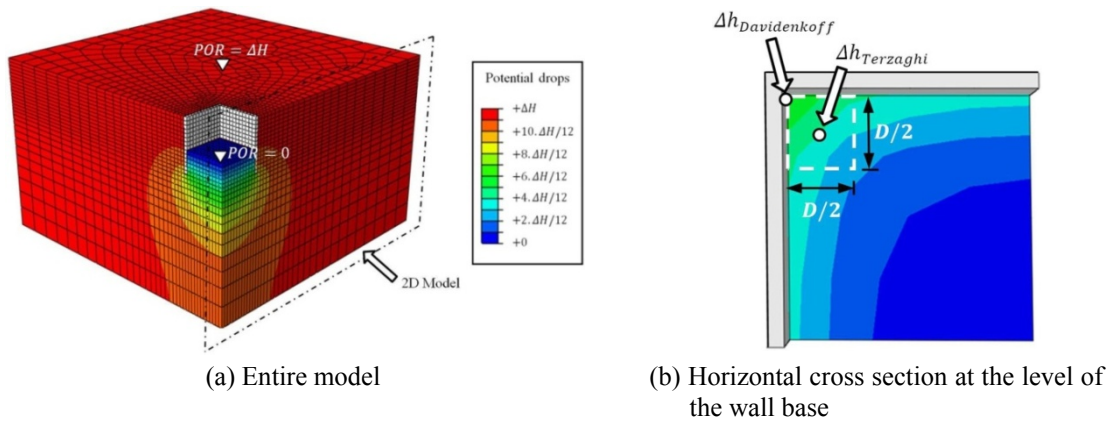


Fig. 4 Equipotential lines (surfaces) for a square shaped excavation pit

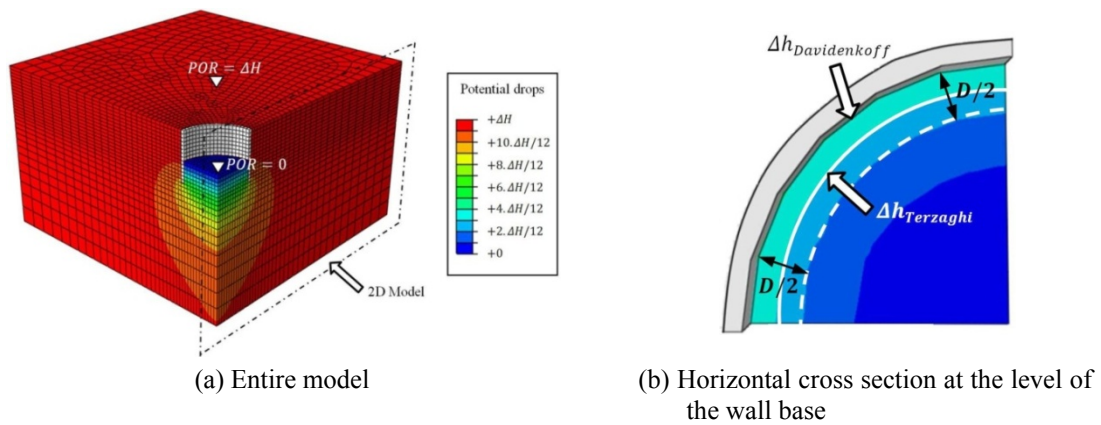


Fig. 5 Equipotential lines (surfaces) for a circular shaped excavation pit

3. Results and discussion

3.1 Seepage failure by heave in homogeneous, isotropic, semi-infinite soils

Groundwater flow concentrates in the corner zones of excavation pits, which is not taken into consideration by using two-dimensional models. Thus, 3D models yield higher hydraulic gradients than 2D models. Figs. 6(a)-(b) show the results of three-dimensional steady-state groundwater flow analyses in respect of the maximum hydraulic gradients occurring on the downstream sides of square and circular shaped sheeted excavation pits in homogeneous, isotropic, semi-infinite soil mediums. The analyses are performed for six various ratios of $\Delta H/D = 0.5, 0.75, 1, 1.25, 1.5, 1.75$ and eight various ratios of $b/D = 0.125, 0.25, 0.5, 1, 2, 4, 6, 8$. As can be seen in Fig. 6, i_{max} decreases with decreasing ratio of $\Delta H/D$ and increasing ratio of b/D . The effect of b/D on hydraulic gradient is negligible for the ratios of $b/D > 2$ in square- as well as for the ratios of $b/D > 4$ in circular- shaped excavation pits.

Fig. 7 illustrates a comparison of the maximum hydraulic gradients obtained from two- and three- dimensional analyses for square- and circular- shaped excavation pits with $\Delta H/D = 1$ and

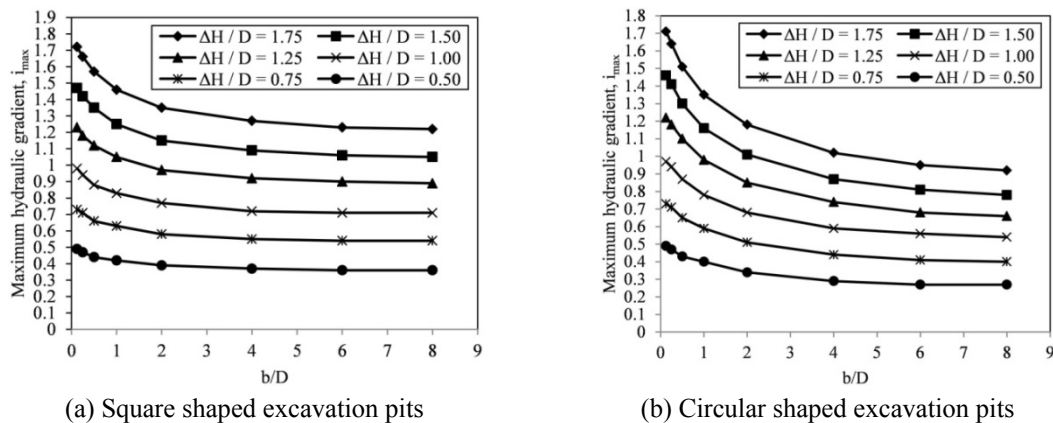


Fig. 6 Maximum hydraulic gradients occurring in a homogeneous, isotropic, semi-infinite soil layer

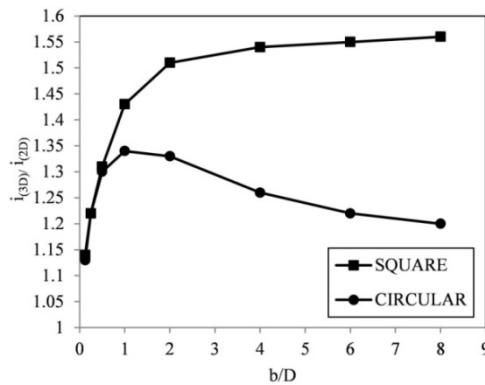


Fig. 7 Comparison of two- and three- dimensional analyses

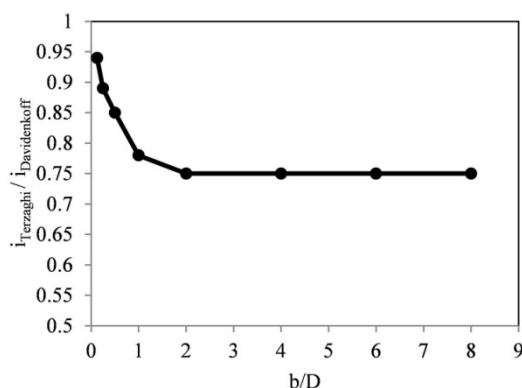


Fig. 8 Comparison of Terzaghi's and Davidenkoff's failure criterions

changing ratios of b/D . As shown in Fig. 7, the difference between the results obtained from 2D and 3D analyses can be too large depending on the ratio of b/D . In square shaped excavation pits, the minimum and maximum ratios of the hydraulic gradients obtained from 3D to those obtained from 2D analyses are 1.14 and 1.56 for $b/D = 0.125$ and $b/D = 8$, respectively. In circular shaped excavations, the ratios lie between 1.13 and 1.34 for $b/D = 0.125$ and $b/D = 1$, respectively. In contrast to square excavation pits, the ratio of i_{3D}/i_{2D} decreases starting from $b/D > 1$, and takes the value of 1.20 for $b/D = 8$. Note that a maximum deviation of $\pm 2.5\%$ in the ratios shown in Fig. 7 can be expected for further ratios of $\Delta H/D$ between 0.5 and 1.75.

3.1.1 Effect of the shape of failure body

Terzaghi's rectangular prism shaped failure body was obtained from two-dimensional model experiments so that its validity is uncertain for three-dimensional groundwater flow analyses. The pore water pressure adjacent to the wall can lift the soil column on the downstream side before a failure occurs according to Terzaghi's criterion. To eliminate this uncertainty, Davidenkoff's method that does not consider any failure body can be used to evaluate seepage failure by heave. It gives the minimum possible safety factor against heave. Furthermore, the use of Davidenkoff's method is on the safe side taking into account the risk of a concentrate flow adjacent to the wall, which may appear especially in loose fine-medium sands with low plasticity silt.

For square shaped excavation pits with $\Delta H/D = 1$ and changing ratios of b/D , the ratios of the average hydraulic gradient determined by using a three-dimensional failure body with the width suggested by Terzaghi for two-dimensional cases to that determined by using an infinitesimal soil column adjacent to the wall are shown in Fig. 8. In the use of Terzaghi's method, the width of the failure body is taken as half of the excavation width when the ratio of $D/2$ is greater than b . The minimum and maximum ratios of $i_{\text{Terzaghi}}/i_{\text{Davidenkoff}}$ are 0.75 and 0.94 for $b/D = 0.125$ and 8, respectively. A maximum deviation of $\pm 1\%$ in the ratios given above can be expected for further ratios of $\Delta H/D$ between 0.5 and 1.75. With the help of Fig. 8, the hydraulic gradients given in Fig. 6 can be converted to those obtained from Terzaghi's method.

3.1.2. Effect of model size

Three-dimensional modeling of groundwater flows may be problematic for large excavation areas due to the limitation of computational power, especially in coupled flow-stress-deformation

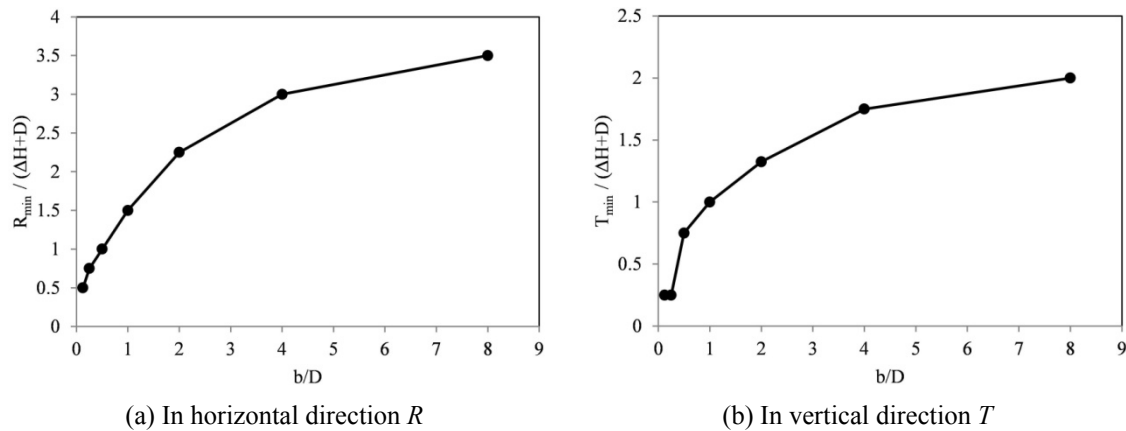


Fig. 9 Required minimum dimensions

analyses. In this case, either the model size or the node number in the numerical model should be reduced.

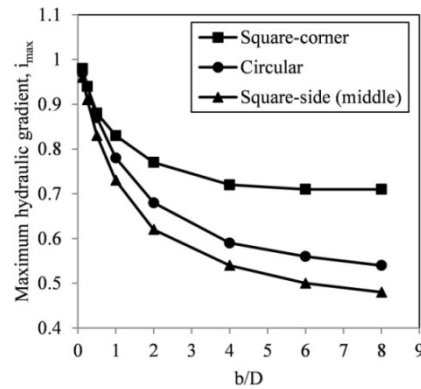
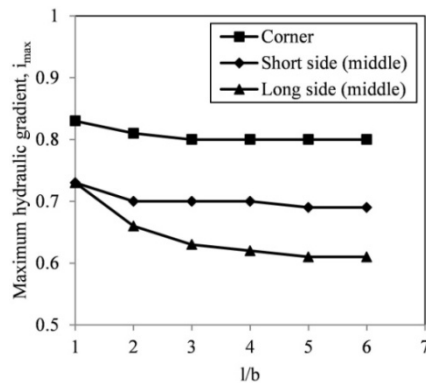
However, it is known that the average hydraulic gradient on the downstream side of an excavation pit increases with increasing horizontal distance from the wall to the outer boundary of the soil model R , and approaches a constant value for a sufficiently large R . The same holds true for the vertical distance from the wall base to the outer boundaries of the soil model T . Hence, the knowledge of the required minimum model size has a great importance with regard to the accuracy of the results of numerical analyses.

For the studied range of $0.5 \leq \Delta H/D \leq 1.75$ and $0.125 \leq b/D \leq 8$, a homogeneous soil layer can be assumed as a semi-infinite layer if it is homogeneous within the dimensions R_{\min} and T_{\min} obtained from Figs. 9(a)-(b). Soil conditions outside these dimensions cause a maximum deviation of $\pm 5\%$ in the hydraulic gradient. As can be seen from Fig. 9, R varies between $0.5(\Delta H+D)$ and $3.5(\Delta H+D)$ while T varies between $0.25(\Delta H+D)$ and $2(\Delta H+D)$ depending on the ratio of b/D .

3.1.3. Effect of the shape of excavation pit

A comparison of maximum hydraulic gradients in square and circular shaped foundation pits with $\Delta H/D = 1$ and changing ratios of b/D is illustrated in Fig. 10. When compared to circular shaped excavations, considerably larger hydraulic gradients arise in square shaped excavations starting from about $b/D \geq 1.5$. The ratios of $i_{\max, \text{square}}/i_{\max, \text{circular}}$ are 1.10 and 1.31 for $b/D = 1.5$ and $b/D = 8$, respectively. A further issue is that the ratio of the hydraulic gradient occurring in the corner zone to the side zone of a square shaped excavation pit becomes significantly large starting from about $b/D = 0.75$. The ratios of $i_{\max(\text{corner})}/i_{\max(\text{side})}$ are 1.10 and 1.48 for $b/D = 0.75$ and $b/D = 8$. Hence, the use of different embedment depths in the corner- and side- zones of square shaped excavations is cost-efficient for large excavation areas.

Fig. 11 illustrates the maximum hydraulic gradients occurring in rectangular shaped excavation pits with $\Delta H/D = 1$, $b/D = 1$ and changing ratios of half of excavation length to half of excavation width l/b . The effect of l/b on the maximum hydraulic gradients in the corner zone and short side-middle is negligibly small so that the risk of heave in rectangular shaped excavation pits can be approximately determined by use of Fig. 6(a). However, the ratio of l/b has a significant effect on i_{\max} in the long side-middle.

Fig. 10 Effect of the shape of excavation pit on i_{max} Fig. 11 Effect of the ratio of l/b on i_{max}

It should be noted that for any shape of an excavation pit whose walls intersect at a right angle, the maximum hydraulic gradient in the corner zone can be also approximated by using Fig. 6(a). In this case, half of the width of the narrowest cross section of the excavation pit should be taken as b .

3.2 Seepage failure by heave in homogeneous, anisotropic, semi-infinite soils

If a homogeneous soil layer is isotropic with respect to permeability, the hydraulic conductivity of the soil layer has no effect on the pore water pressure distribution in the flow region, and therefore, no effect on quick condition (see Eq. (5)). However, if the horizontal permeability of the soil layer is greater than the vertical permeability, a larger pore water pressure occurs on the downstream side when compared to isotropic case.

Experimental and theoretical investigations showed that due to the flatness and orientation of grains, the ratio of the hydraulic conductivity in the horizontal direction to that in the vertical direction k_h/k_v cannot be greater than 2.5 even for very flat particles and well pronounced orientation (Witt and Brauns 1983). In a further study, a series of permeability tests on high-quality undisturbed coarse grained soil samples was performed using a triaxial cell. The

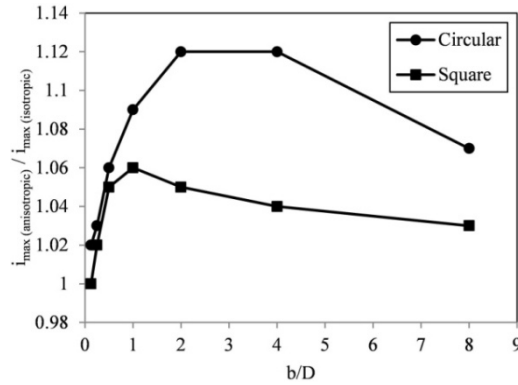


Fig. 12 Effect of anisotropic permeability on i_{max}

undisturbed soil samples were recovered by the in-situ freezing sampling method. Based on the test results, it is found that the maximum ratio of k_h/k_v is 1.7 (Hatanaka *et al.* 1997). Clennell *et al.* (1999) stated that, in natural clays, permeability anisotropy produced by consolidation is in the range 1.1-3, and does not reach the high levels predicted by simple models of clay particle reorientation.

Fig. 12 demonstrates the influence of anisotropic permeability on the maximum hydraulic gradients for excavation pits with $\Delta H/D = 1$ and changing ratios of b/D . The maximum ratios of hydraulic gradients obtained in the case of anisotropic permeability ($k_h/k_v = 3$) to those in the case of isotropic permeability ($k_h/k_v = 1$) are 1.06 and 1.12 for square and circular shaped excavations, respectively. The numerical analyses performed for further ratio of $\Delta H/D$ between 0.5 and 1.75 showed a maximum deviation of $\pm 2.5\%$ in the ratios given above.

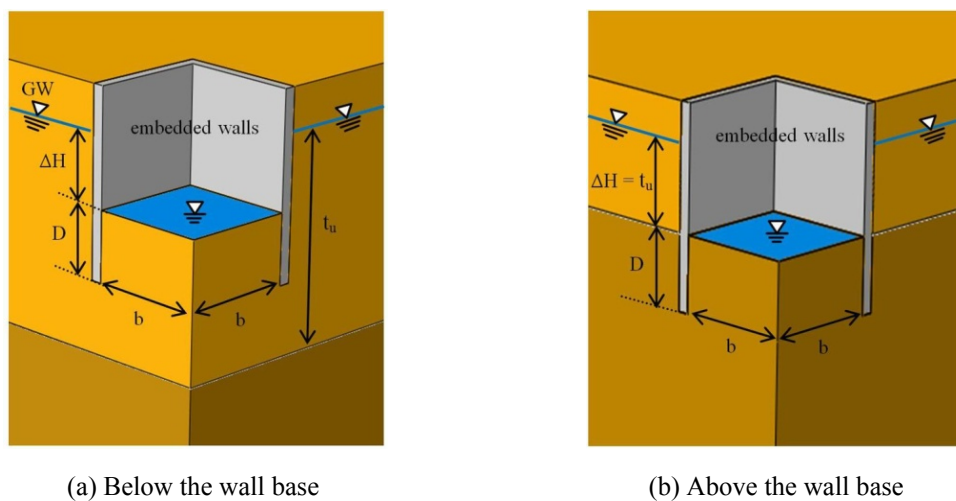


Fig. 13 Seepage failure by heave in the case of horizontal stratification

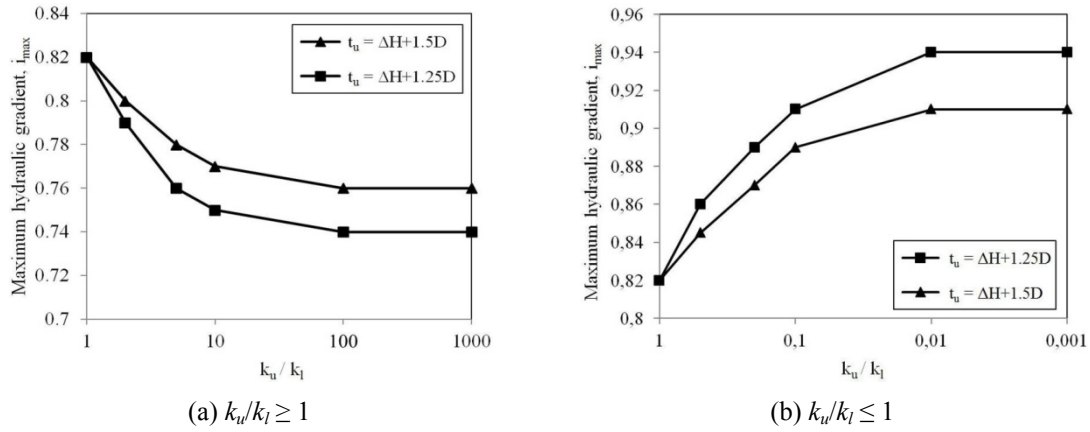


Fig. 14 Effect of horizontal stratification below the wall base

3.3 Seepage failure by heave in stratified soils

To investigate the seepage failure by heave in stratified soils, it is distinguished between a horizontal stratification below the wall base and a horizontal stratification above the wall base, as shown in Figs. 13(a)-(b). The horizontal distance from the wall to the outer boundary of the soil model and the thickness of the lower soil layer are chosen such that their effects on i_{max} are negligibly small. The groundwater level within the excavation pit, which is shown with the blue-colored surface, lies on the excavation base.

3.3.1 Effect of horizontal stratification below wall base

The influence of a horizontal stratification below the wall base on the maximum hydraulic gradient is presented in Fig. 14 for a square shaped excavation pit with $\Delta H/D = 1$ and $b/D = 1$. The investigations are performed for two various thicknesses of the upper soil layer below the groundwater level, namely for $t_u = \Delta H + 1.25D$ and $t_u = \Delta H + 1.5D$. The ratio of the hydraulic conductivity of the upper soil layer to the hydraulic conductivity of the lower layer is varied as $k_u/k_l = 1/1000, 1/100, 1/10, 1/5, 1/2, 1, 2, 5, 10, 100, 1000$.

It is apparent from Fig. 14(a) that a horizontal stratification within the required minimum vertical distance T_{min} , which can be obtained from Fig. 9(b), leads to a smaller hydraulic gradient than that in homogeneous case when the upper layer is more permeable than the lower layer. The maximum hydraulic gradient decreases with increasing ratio of k_u/k_l , and increases with increasing t_u . The maximum hydraulic gradient should finally reach the value in the homogeneous case when the thickness of the upper soil layer below the groundwater level is sufficiently large, in other words, the top surface of the lower layer has a sufficient distance from the wall base. Hence, the presence of a relatively less permeable soil layer below the wall base is important for cost-efficient design against heave.

In the case that the upper layer is less permeable than the lower layer, a horizontal stratification within the required minimum vertical distance T_{min} causes a larger hydraulic gradient than that in the homogeneous case, as shown in Fig. 14(b). The maximum hydraulic gradient decreases with increasing t_u , and increases with decreasing ratio of k_u/k_l . Finally, the maximum hydraulic gradient should reach the value in the homogeneous case when the top surface of the lower layer has a

sufficient distance from the wall base. Therefore, the presence of a relatively more permeable soil layer below the wall base is important for safety design against heave.

3.3.2 Effect of horizontal stratification above wall base

Two cases are examined to illustrate the influence of a horizontal stratification above the wall base on seepage failure by heave. In the first case, a relatively more permeable soil layer is considered as upper layer whereas a less permeable soil layer is the upper layer in the second case. The thickness of the upper soil layer below the groundwater level is varied as $t_u = \Delta H, \Delta H + 0.25D, \Delta H + 0.5D, \Delta H + 0.75D$.

To evaluate the risk of heave, two hydraulic gradients $i_{interface}$ and i_{tip} are determined according to Daidenkoff’s method. They are calculated by using Eqs. (6)-(7).

$$i_{interface} = \frac{\Delta h_{interface}}{D_u} \tag{6}$$

$$i_{tip} = \frac{\Delta h_{tip}}{D} \tag{7}$$

where $\Delta h_{interface}$ is the hydraulic head difference between the interface of the soil layers and the excavation base, D_u is the thickness of upper soil layer below excavation base, Δh_{tip} is the hydraulic head difference between the wall tip and the excavation base, D is the embedment depth of the wall.

Tables 1-2 present the influence of a horizontal stratification above the wall base for a wide ($b/D = 4$) and a narrow ($b/D = 0.25$) square shaped excavation pit with $\Delta H/D = 1$ in the case that the upper soil layer is more permeable than the lower layer. The ratio of the hydraulic conductivity of the upper layer to the hydraulic conductivity of the lower soil layer is varied as $k_u/k_l = 1, 2, 5, 10, 100, 1000$.

It is apparent from Tables 1-2 that the maximum hydraulic gradient appears at the wall tip in all cases, and the effect of the location of the interface surface on i_{tip} can be ignored. Namely, the effect of the location of the interface surface on the decrease of i_{tip} is lower than 10% so long as the thickness of the upper soil layer is not greater than $\Delta H + 0.75D$, especially for $b/D = 0.25$. Although the ratio of k_u/k_l has a considerable effect on $i_{interface}$, its effect on i_{tip} can be also neglected.

Table 1 Hydraulic gradients for $\Delta H/D = 1, b/D = 4$ in the case of $k_u/k_l \geq 1$

k_u/k_l	Thickness of upper soil layer, t_u							
	$t_u = \Delta H$		$t_u = \Delta H + 0.25D$		$t_u = \Delta H + 0.5D$		$t_u = \Delta H + 0.75D$	
	i_{tip}	i_{tip}	$i_{interface}$	i_{tip}	$i_{interface}$	i_{tip}	$i_{interface}$	
1	0.72	0.72		0.72		0.72		
2	0.75	0.75	0.31	0.74	0.34	0.74	0.43	
5	0.77	0.76	0.13	0.75	0.17	0.75	0.24	
10	0.77	0.77	0.06	0.76	0.09	0.76	0.14	
100	0.77	0.77	0	0.77	0.01	0.77	0.02	
1000	0.78	0.78	0	0.77	0	0.77	0	

Table 2 Hydraulic gradients for $\Delta H/D = 1$, $b/D = 0.25$ in the case of $k_u/k_l \geq 1$

k_u/k_l	Thickness of upper soil layer, t_u							
	$t_u = \Delta H$		$t_u = \Delta H + 0.25D$		$t_u = \Delta H + 0.5D$		$t_u = \Delta H + 0.75D$	
	i_{tip}	i_{tip}	$i_{interface}$	i_{tip}	$i_{interface}$	i_{tip}	$i_{interface}$	
1	0.93	0.93		0.93		0.93		
2	0.93	0.92	0.49	0.92	0.56	0.91	0.64	
5	0.93	0.92	0.21	0.90	0.27	0.88	0.37	
10	0.93	0.92	0.10	0.90	0.14	0.87	0.22	
100	0.93	0.92	0.01	0.89	0.01	0.85	0.03	
1000	0.93	0.92	0	0.89	0	0.85	0	

When compared to homogeneous case, a horizontal stratification with $k_u/k_l \geq 1$ has negligible effect on i_{tip} .

It should be noted that a relatively more permeable, upper soil layer can induce a significantly larger critical hydraulic gradient than that calculated, provided that its pores are fine enough to prevent the transport of the particles of lower soil layers. The reason for the increase in the critical gradient is the large difference between i_{tip} and $i_{interface}$. Namely, the upper layer retains its strength even though the effective stresses within the lower soil layer become zero. As a result, the friction forces occurring within the upper layer prevent an eventual failure at the theoretical critical hydraulic gradient (Odenwald and Herten 2008).

Tables 3-4 indicate the effect of a horizontal stratification on hydraulic heave for a wide and a narrow square shaped excavation pit with $\Delta H/D = 1$ in the case that the upper layer is less permeable than the lower layer. The ratio of the hydraulic conductivity of the upper layer to the hydraulic conductivity of the lower soil layer is varied as $k_u/k_l = 1, 1/1.25, 1/1.50, 1/1.75, 1/2, 1/5, 1/10, 1/100, 1/1000$.

Table 3 Hydraulic gradients for $\Delta H/D = 1$, $b/D = 4$ in the case of $k_u/k_l \leq 1$

k_u/k_l	Thickness of upper soil layer, t_u					
	$t_u = \Delta H$		$t_u = \Delta H + 0.25D$		$t_u = \Delta H + 0.5D$	
	i_{tip}	i_{tip}	$i_{interface}$	i_{tip}	$i_{interface}$	
1	0.72	0.72		0.72		
1/1.25	0.72	0.73	0.64	0.73	0.64	
1/1.50	0.71	0.73	0.73	0.73	0.70	
1/1.75	0.71	0.73	0.81	0.74	0.76	
1/2	0.70	0.73	0.89	0.74	0.81	
1/5	0.65	0.73	1.49	0.77	1.14	
1/10	0.61	0.75	2.03	0.82	1.39	
1/100	0.46	0.93	3.51	0.95	1.88	
1/1000	0.20	0.98	3.91	0.99	1.98	

Table 4 Hydraulic gradients for $\Delta H/D = 1$, $b/D = 0.25$ in the case of $k_u/k_l \leq 1$

k_u/k_l	Thickness of upper soil layer, t_u				
	$t_u = \Delta H$	$t_u = \Delta H + 0.25D$		$t_u = \Delta H + 0.5D$	
	i_{tip}	i_{tip}	$i_{interface}$	i_{tip}	$i_{interface}$
1	0.93	0.93	0.93	0.93	0.93
1/1.25	0.93	0.93	1.03	0.94	0.99
1/1.50	0.93	0.94	1.19	0.94	1.09
1/1.75	0.93	0.94	1.32	0.95	1.16
1/2	0.93	0.94	1.45	0.95	1.22
1/5	0.93	0.96	2.37	0.97	1.60
1/10	0.93	0.97	2.98	0.99	1.79
1/100	0.90	0.99	3.92	1.00	2.00
1/1000	0.70	1.00	4.05	1.00	2.02

A horizontal stratification ($k_u/k_l \leq 1$) above the excavation base causes a smaller hydraulic gradient than that in homogeneous case, and the most favorable case appears when the upper layer thickness t_u is equal to ΔH , especially in the wide excavation pit. This favorable effect is visible in the narrow excavation pit only when the ratio of k_u/k_l is greater than 1/100. However, it should be noted that this favorable effect should be considered only when the upper soil layer is continuous within a sufficiently large, horizontal distance from the wall on the upstream side.

An even greater thickness of the upper layer, namely a horizontal stratification between the excavation base and the wall tip induces a greater hydraulic gradient than that in homogeneous case. In this case, except for $b/D = 4$ and $k_u/k_l \leq 1/1.5$, the maximum hydraulic gradient arises at the interface of the soil layers so that the upper layer is more vulnerable than the lower layer with respect to seepage failure by heave. The hydraulic gradient at the interface of the soil layers increases with decreasing ratio of k_u/k_l and decreasing thickness of the upper soil layer t_u .

As can be seen from Tables 3-4, a decrease in the thickness of the upper layer from $\Delta H + 0.5D$ to $\Delta H + 0.25D$ leads to a large increase in the maximum hydraulic gradient at the interface surface depending on the ratio of k_u/k_l . Thus, the presence of an inclined stratification can be a considerable effect on $i_{interface}$ depending on its inclination angle and the width as well as the length of the excavation pit.

A further issue is that a small decrease of the ratio of k_u/k_l induces a significant increase in $i_{interface}$, especially in narrow excavation pits. For instance, the ratio of $k_u/k_l = 1/1.5$ leads to an increase of $i_{interface}$ about 28% for $\Delta H/D = 1$, $b/D = 0.25$ and $t_u = \Delta H + 0.25D$ when compared to the homogeneous case. The accuracy of hydraulic conductivities obtained from laboratory tests depends on how well the content and structure of soil samples represent the natural state of the soil (Bandini and Sathiskumar 2009). However, it is difficult to obtain undisturbed samples from cohesionless soils, and it is not faultless to estimate the relative densities of this type of soils from field penetration tests (Hamidi *et al.* 2013). Additionally, the determination of maximum and minimum density of gap-graded soils (soils containing many large particles with limited small particles) is also difficult due to segregation appearing during sample preparation. Moreover, gap graded soils are unsafe with regard to suffusion. In other words, the transport and redistribution of fine grains start at a hydraulic gradient much lower than i_{cr} , which results in the change of the

hydraulic conductivities of soil layers in course of time (Skempton and Brogan 1994, Ke and Takahashi 2012).

Finally, it should be mentioned that the thicknesses and hydraulic conductivities of soil layers are available in the case of macro-stratification. However, many natural sedimentary deposits contain thin soil bands. When compared to the cases mentioned above, a relatively less permeable, thin soil band between the excavation base and the wall tip within a homogenous soil medium leads to even greater hydraulic gradients. In this case, most of head loss takes place within the thin soil band. Namely, the maximum hydraulic gradient occurs at the bottom level of the thin soil band. To detect the presence of such thin layers, in-situ pumping test is a very useful tool. The most dangerous situation appears when such a thin soil layer is not continuous within a sufficiently large, horizontal distance from the wall on the upstream side. The most reliable is to carry out pore water pressure measurements during construction phases.

4. Conclusions

Based on the results of finite element analyses of steady state groundwater flow into sheeted excavation pits with $0.5 \leq \Delta H/D \leq 1.75$ and $0.125 \leq b/D \leq 8$, the following conclusions have been achieved with regard to seepage failure by heave:

In homogeneous semi-infinite soils;

- Depending on the ratio of b/D , the ratios of maximum hydraulic gradients obtained from 3D to those obtained from 2D analyses vary from 1.14 to 1.56 and 1.13 to 1.34 for square and circular shaped excavation pits, respectively.
- Depending on the ratio of b/D , the ratio of the average hydraulic gradient determined according to Terzaghi's method to that determined according to Baumgart & Davidenkoff's method varies between 0.75 and 0.94.
- Taking into account three-dimensional groundwater flow, the maximum hydraulic gradient on the downstream side of a square or circular shaped excavation pit can be found out with the help of Fig. 6.
- When compared to circular excavations, a considerably larger hydraulic gradient arises in square shaped excavations, especially when the ratio of b/D is equal to or more than 1.5. The difference between the maximum hydraulic gradients occurring in the corner zones of rectangular and square shaped excavations is negligibly small for the same ratios of b/D and $\Delta H/D$.
- When compared to isotropic case, anisotropic permeability ($k_h/k_v = 3$) leads to an increase in the hydraulic gradient of up to 6% and 12% for square and circular shaped excavation pits, respectively.

In stratified soils;

An upper layer that is less permeable than the lower layer has a great effect on seepage failure by heave. In this case, the most favorable case appears when the interface surface of the soil layers is located above the excavation base while the most unfavorable case appears when the interface surface is located between the excavation base and the wall base. When compared to homogeneous case, an upper layer that is more permeable than the lower layer has negligible effect on the hydraulic gradient at wall tip as long as the thickness of the upper soil layer is not greater than ΔH

+ 0.75D. A horizontal stratification below the wall base can lead to a significant increase or decrease in the hydraulic gradient depending on the ratio of the hydraulic conductivity of upper soil layer to lower soil layer and the distance of the lower soil layer from the wall base.

References

- Aulbach, B. and Ziegler, M. (2013), "Simplified design of excavation support and shafts for safety gainst hydraulic heave", *Geomech. Tunn.*, **6**(4), 362-374.
- Aulbach, B. and Ziegler, M. (2014), "Versagensform und Nachweisformat beim hydraulischen Grundbruch-Plädoyer für den Terzaghi-Körper", *Geotechnik*, **37**(1), 6-18.
- Bandini, P. and Sathiskumar, S. (2009), "Effect of silt content and void ratio on the saturated hydraulic conductivity and compressibility of sand-silt mixtures", *J. Geotech. Eng.*, **135**(12), 1976-1980.
- Benmebarek, N., Benmebarek, S. and Kastner, R. (2005), "Seepage failure of sand within a cofferdam", *Comput. Geotech.*, **32**(4), 264-273.
- Cai, F., Ugai, K., Takahashi, C., Nakamura, H. and Okaki, I. (2004), "Seepage analysis of two case histories of piping induced by excavations in cohesionless soils", *Proceedings of the First International Conference on Construction IT*, Beijing, China, August.
- Clennell, M.B., Dewhurst, D.N., Brown, K.M. and Westbrook, G.K. (1999), *Permeability Anisotropy of Consolidated Clays*, Geotechnical Society Special Publication, No. 158, pp. 79-96.
- Das, B.M. (2008), *Advanced Soil Mechanics*, Taylor & Francis Group, London / New York.
- Davidenkoff, R. (1970), *Unterläufigkeit von Stauwerken*, Werner Verlag, Düsseldorf, Germany.
- Davidenkoff, R.N. and Franke, O.L. (1965), "Untersuchung der räumlichen Sickerströmung in eine umspundete Baugrube in offenen Gewässern", *Bautechnik*, **42**(9), 298-306.
- EAB (2008), Recommendations on excavations, Ernst & Sohn - Wiley, Berlin, Germany.
- EAU (2004), Recommendations of the committee for waterfront structures, harbours and waterways, Ernst & Sohn - Wiley, Berlin, Germany.
- EN 1997-1: Eurocode 7 (2004), Geotechnical design - Part 1: General rules, European Committee for Standardisation, Brussels, Belgium.
- Fellin, W., Kellermann, F. and Wilhelm, T. (2003), "Der Einfluss von Kanalbildungen auf die hydraulische Grundbruchsicherheit", *Österreichische Ingenieur- und Architekten Zeitschrift*, **148**(2), 42-47.
- Ghiassian, H. and Ghareh, S. (2008), "Stability of sandy slopes under seepage conditions", *Landslides*, **5**(4), 397-406.
- Hamidi, B., Varaksin, S. and Nikraz, H. (2013), "Relative density concept is not a reliable criterion", *Proceedings of the ICE-Ground Improvement*, **166**(4), 196-208.
- Harr, M.E. (1962), *Groundwater and Seepage*, McGraw Hill Publishing Co., Inc., New York, NY, USA.
- Harza, L.F. (1935), "Uplift and seepage under dams in sand", *Trans. Am. Soc. Civ. Eng.* **100**(1), 1352-1385.
- Hatanaka, M., Uchida, A. and Takehara, N. (1997), "Permeability characteristics of high - quality undisturbed sands measured in a triaxial cell", *Soil. Found.*, **37**(3), 129-135.
- Hiroso, T. and Tanaka, T. (2007), "A case study on seepage failure of excavated bottom soil in a steel-sheet-pile-wall cofferdam", *T. Jpn. Soc. Irrig. Drain. Reclam. Eng.*, **75**(2), 145-156.
- Kaiser, P.K. and Hewitt, K.J. (1982), "The effect of groundwater flow on the stability and design of retained excavations", *Can. Geotech. J.*, **19**(2), 139-153.
- Ke, L. and Takahashi, A. (2012), "Strength reduction of cohesionless soil due to internal erosion induced by one dimensional upward seepage flow", *Soil. Found.*, **52**(4), 698-711.
- Lee, I.M. and Nam, S.W. (2001), "The study of seepage forces acting on the tunnel lining and tunnel face in shallow tunnels", *Tunn. Undergr. Space Technol.*, **16**(1), 31-40.
- Marsland, A. (1953), "Model experiments to study the influence of seepage on the stability of a sheeted excavation in sand", *Geotechnique*, **3**(6), 223-241.
- McNamee, J. (1949), "Seepage into a sheeted excavation", *Geotechnique*, **1**(4), 229-241.

- Odenwald, B. and Herten, M. (2008), "Hydraulischer Grundbruch: neue Erkenntnisse", *Bautechnik*, **85**(9), 585- 595.
- Reddi, L.M. (2003), *Seepage in Soils: Principles and Applications*, John Wiley & Sons, Inc., NJ, USA.
- Schmitz, S. (1990), "Hydraulische Grundbruchsicherheit bei räumlicher Anströmung", *Bautechnik*, **67**(9), 301-307.
- Skempton, A.W. and Brogan, J.M. (1994), "Experiments on piping in sandy gravels", *Geotechnique*, **44**(3), 449-460.
- Tanaka, T. and Verruijt, A. (1999), "Seepage failure of sand behind sheet piles. The mechanism and practical approach to analyse", *J. Jpn. Geotech. Soc. Soil. Found.*, **39**(3), 27-35.
- Tanaka, T., Song, S., Shiba, Y., Kusumi, S. and Inoue, K. (2012), "Seepage failure of sand in three dimensions-experiments and numerical analyses", *Proceedings of the 6th International Conference on Scour and Erosion*, Paris, France, August.
- Terzaghi, K. (1925), *Erdbaumechanik auf bodenphysikalischer Grundlage*, Franz Deuticke-Verlag, Leipzig/Wien.
- Terzaghi, K. and Peck, R.B. (1948), *Soil Mechanics in Engineering Practice*, John Wiley & Sons, New York, NY, USA.
- Witt, K.J. and Brauns, J. (1983), "Permeability – anisotropy due to particle shape", *J. Geotech. Eng.*, **109**(9), 1181-1187.
- Wudtke, R.B. and Witt, K.J. (2006), "A static analysis of hydraulic heave in cohesive soil", *Proceedings of the 3rd International Conference on Scour and Erosion*, Amsterdam, Netherlands, November.
- Yang, X.L. and Qin, C.B. (2014), "Limit analysis of rectangular cavity subjected to seepage forces based on Hoek-Brown failure criterion", *Geomech.Eng., Int. J.*, **6**(5), 503-515.
- Zheng, G. and Yang, J. (2011), "Analysis of the formula for checking the heaving stability of excavations", *China Civil Eng. J.*, **44**(2), 123-127.
- Ziegler, M., Aulbach, B., Heller, H. and Kuhlmann, D. (2009), "Der Hydraulischer Grundbruch – Bemessungsdiagramme zur Ermittlung der erforderlichen Einbindetiefe", *Bautechnik*, **86**(9), 529-541.